Cardiac MRI Intervention and Diagnosis via Deformable Collaborative Tracking

Yan Zhou, Nikolaos V. Tsekos, and Ioannis T. Pavlidis

Department of Computer Science, University of Houston, Houston, TX 77024, USA

Abstract. The high contrast and lack of ionizing radiation, renders Magnetic Resonance Imaging (MRI) a suitable modality for continuous intra-operative imaging. Tracking the motion of key locations in cardiac MRI is of paramount importance in control and guidance in emerging robot-assisted interventions. Tracking can also be used to assess myocardial wall motion for diagnostic purposes. This article presents an expanded collaborative tracking algorithm to facilitate both interventions and diagnosis in MRI. Specifically, the network of trackers not only follows anatomical landmarks on the beating heart but also computes its evolving deformable surface on a specific plane. Experimental investigations with both CINE and real-time MRI demonstrate that the collaborative tracker network achieves robust real-time performance over long periods, outperforming the MIL tracker. Pilot experimental results also demonstrate that the evolution of the network's deformation mesh can be used for blood volume estimation and computation of the ejection fraction - both of great diagnostic value.

1 Introduction

Image-guided robot-assisted interventions promise to improve patient management and reduce the cost of delivered health care. Real-time tracking of cardiac anatomical landmarks is paramount in such intra-operative interventions to maneuver the robotic manipulator around critical tissue. A major drawback of legacy procedures is that the anatomical information is not updated intra-operatively. Hence, any tissue shifts induced by the advancement of the interventional tools cannot be compensated for. Tissue dislocations are difficult to predict as they depend on tissue elastic properties and the speed of advancement [1][2][3][4][5][6]. Moreover, conventional MRI guided procedures that entail the insertion of the tool while the patient is outside the scanner followed by validating scanning, become lengthy and cause additional discomfort to the patient. They may also result to more surgical trauma and increased chances for complications due to multiple insertion attempts.

To keep track of a specific anatomical landmark over time, one approach is to segment the underlying structures in each slice. Such approach may entail defining an appropriate optimization scheme to iteratively minimize a cost function, and the computational cost can be significant. For example, in [7], while the proposed boundary segmentation method achieved very high accuracy, the computational time was 10 seconds per slice. In contrast, Yuen et al. [8] achieved

D.N. Metaxas and L. Axel (Eds.): FIMH 2011, LNCS 6666, pp. 188–194, 2011.

real-time performance in Ultrasound images with an extended Kalman filter tracker. Zhou et al. [9] proposed to use multiple particle filter trackers to track a single region. For each tracker, a decision is made to classify it as "survivor" or "failed". Tracker interaction is modeled via a Bayesian network. The approach is able to achieve accurate overall state estimation in real-time, as an evidence for the motion estimation of a specific landmark point.

In this article we extend Zhou's method to handle tissue surface deformation and not just motion of single landmark points. Different trackers in the network may have different motion patterns due to non-linear tissue deformation. This motivates to take advantage of each tracker's specific location, and form a deformation mesh. The deformed region captures the heart's surface undergoing non-linear deformations. The surface area from the deformation mesh shows periodical rhythm during heart's contraction and extraction - a feature that may be used in diagnosis. We also compare our approach to the state-of-art Multiple Instance Learning (MIL) tracker [10]. MIL tracker uses an online-boosting approach to train the appearance model at each time step. And the training examples are presented in "bags" rather than individual instances. The experimental results show that although MIL tracker captures abrupt motion and appearance changes at first, it gradually drifts and finally loses the target as time passes by. Our tracking approach outperforms the MIL tracker both in speed and robustness in long tracking sequences.

In section 2 we describe in detail the methodological approach. In section 3 we present analysis of the experimental performance of the method.

2 Methodology

2.1 Collaborative Tracking

We have adopted as a baseline methodology the collaborative tracking algorithm proposed by Zhou et al. [9]. The algorithm tracks the region of interest via a grid of particle filter trackers. After each tracker's motion state is estimated as an independent particle filter tracker, the tracker network is formed. For each individual tracker T_i in the 3×3 grid, a decision is made whether to include it or not into the survivor group. The adjacent trackers $\{T_j, ..., T_m\}$ provide evidence to make this decision via a Bayesian network.

$$p(W_{i,t}, \hat{\Theta}_{i,t} | G_{i,t-1}, Z_{i,t}) \propto p(G_{i,t-1}) \prod_k N(\hat{\theta}_{i,t} | \hat{\theta}_{k,t}, \sigma^2) \prod_k p(\hat{\theta}_{k,t} | z_{k,t}). \quad (1)$$

The surviving probability of $T_{i,t}$ is computed in Equation (1); please note that $\hat{\Theta}_{i,t} = \{\hat{\theta}_{i,t}, \hat{\theta}_{j,t}, ..., \hat{\theta}_{m,t}\}$ and $Z_{i,t} = \{z_{i,t}, z_{j,t}, ..., z_{m,t}\}$ are the estimated states and observations of T_i and its adjacent trackers at time t. $W_{i,t}$ represents the event that tracker T_i is in the survivor group at time t. $G_{i,t-1}$ is the Bayesian network at time $t-1$, whose probability $p(G_{i,t-1})$ is known at time t. $N(\hat{\theta}_{i,t} | \hat{\theta}_{k,t}, \sigma^2)$ is the probability density of $\hat{\theta}_{i,t}$ on the Normal distribution centered at $\hat{\theta}_{k,t}$ with variance σ^2.

$p(W_{i,t}, \hat{\Theta}_{i,t}|G_{i,t-1}, Z_{i,t})$ serves as evidence in deciding whether to include or not tracker T_i in the survivor group. If the evidence exceeds a certain threshold (0.05 in our implementation), then it is included in the survivor group, otherwise it is excluded.

The overall motion state is determined by the trackers in the survivor group and computed as follows:

$$\hat{\theta}_{overall} = \frac{1}{\sum_{i=1}^{|W|} \beta_i} \sum_{i=1}^{|W|} \hat{\theta}_i \beta_i, \tag{2}$$

where $|W|$ is the cardinality of the survivor group and β_i is the impact factor of each linked tracker. The latter is determined from:

$$\beta_i = \frac{p(W_{i,t}, \hat{\Theta}_{i,t}|G_{i,t-1}, Z_{i,t})}{D_{i,t}}, \tag{3}$$

where the enumerator is the conditional probability computed in Equation (1) and $D_{i,t}$ is the Euclidean distance from the point of interest (landmark) to the center of the tracker.

2.2 Deformed Region Computation

The multi-tracker network concept presented in [9] is quite powerful but is grossly underutilized. It is used to track single landmark points in cardiac MRI. Here we expand the algorithm to perform deformation mesh computation and track tissue surfaces, not just points.

Specifically, we compute the deformation mesh out of all the surviving trackers in the network. The deformation mesh M_t is composed of a set of nodes $c = (c_1, c_2, ..., c_n)$, which are distributed over the selected target region during the initialization step. Each node is linked to several trackers (Figure 1) and its location is decided by the linked survivor trackers as described in Equation (4):

$$c_i = \frac{1}{\sum_{k=1}^{u_i} \beta_k} \sum_{k=1}^{u_i} p_k \beta_k, \tag{4}$$

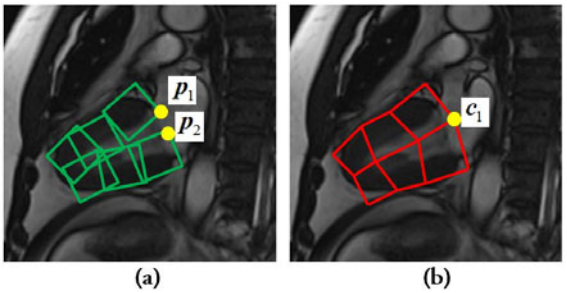

Fig. 1. Deformation mesh computation: (a) Survivor group is selected and colored in green. (b) Computed deformation mesh.

where $\{p_k\}_{k=1}^{u_i}$ indicates all the corner coordinates of the linked survivor trackers at a certain location and β_k is the impact factor of each linked tracker; u_i is the total number of surviving trackers. We use the conditional probability computed in Equation (1) as the impact factor here.

The deformation mesh follows the heart surface while undergoing non-linear tissue deformations. The surface region contracts and expands periodically with the beating heart. This motivates us to examine the surface area of the deformation mesh, which is computed in Equation (5): $polyArea(M_t)$ is the polygon area covered by the deformation mesh, and u_i is the total number of surviving trackers. Experiments in Section 3.2 demonstrate the potential applications of the mesh's evolution.

$$surf = \frac{polyArea(M_t)}{u_i} \tag{5}$$

3 Experimentation

In this study we compare the performance of the collaborative tracker [9] with that of MIL [10] in tracking landmarks in long cardiac MRI sequences. This is in contrast to the short sequences reported in [9], where no comparison was attempted. This part of the experimentation solidifies the baseline algorithm' potential in interventional MRI. Furthermore, we present initial experimental results regarding the computation of cardiac function out of the evolution of the deformation mesh - an algorithmic extension introduced in the present article. This is a development with great diagnostic potential.

3.1 Collaborative versus MIL Tracking in Interventional MRI

The MIL [10] tracking code was downloaded from the authors' webpage. Figure 2 shows a sample visualization from the comparative study. The MRI sequence used in testing consists of 60 repeating cycles, and each cycle includes 25 frames of short-axis view images. The entire sequence has a total of 1500 frames, and lasts 1 minute. Each column shows one snapshot from the tracking sequence by different approaches. The first row shows snapshots of the deformation mesh's evolution as computed by the collaborative tracker. The second row shows the corresponding anatomical landmark locations as computed by the collaborative tracker. The third row shows the corresponding anatomical landmark locations as computed by the MIL tracker. One can observe that the MIL tracker performs well at first, but gradually it drifts to other locations. This could be a fatal problem in interventional MRI, where the operation is expected to last several minutes. A likely reason for the drift is that MIL constantly updates its appearance template through an online-boosting approach. Although this boosting method uses a bag of appearance patches, it is fuzzy about how the exact appearance of the target during evolution; consequently, small errors start accumulating with time. On the contrary, the collaborative tracker, thanks to its redundancy, achieves stable results, which is paramount in robotic interventions.

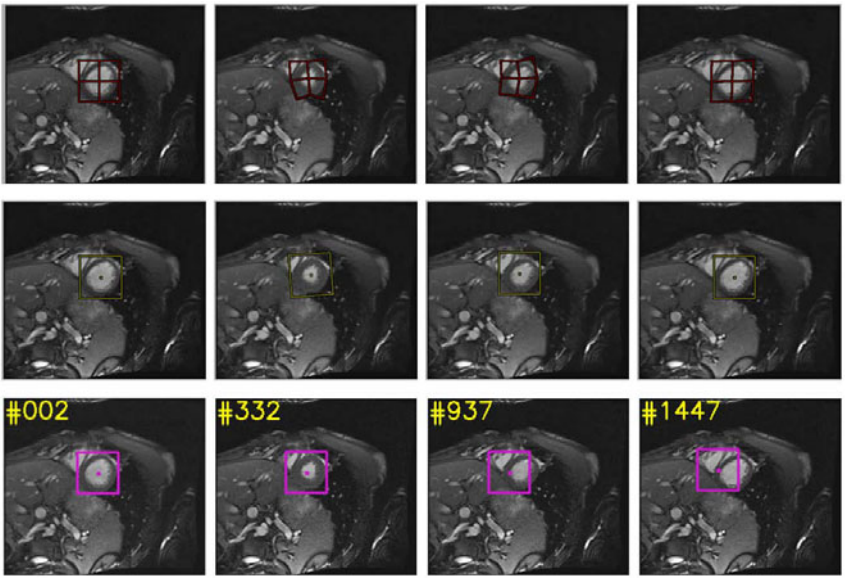

Fig. 2. Comparison results with MIL tracker

Despite this redundancy, the collaborative tracker remains highly efficient and achieves 28 fps on a standard PC versus the 9 fps of the MIL tracker. This has to do with the simple nature of the individual particle filter trackers in the network. Hence, the collaborative tracker renders itself to real-time implementation.

3.2 Surface Area Computation

We computed the evolved area of the deformation mesh and formed respective signals. We applied this analysis on two data sets: the CINE (Figure 3) and the single axis ultrafast dynamic cardiac MRI (Figure 4).

Results from a representative CINE set are shown in Figure 3; the signal clearly tracks the cardiac cycle. One can discern the rapid squeeze of the heart during systole (the lower peak), then the recovery of the relaxing myocardium, and finally reaching the end-diastolic phase (the highest peak). Such dynamic pattern was observed in all slices and subjects we studied.

Results from a sequence with 1350 images at a speed of 50 ms/slice are shown in Figure 4. In this case the same single slice was collected for a far longer period as compared to the CINE sequence in Figure 3. Although, Figure 4 illustrates the same periodicity, because it does not have the time resolution of CINE it does not provide us with the same high resolution assessment of the heart phase changes. In addition, the maxima (end-diastole) and the minima (end-systole) are not as regular as it would be been expected, due to highly varying contrast encountered in such rapid continuous acquisitions.

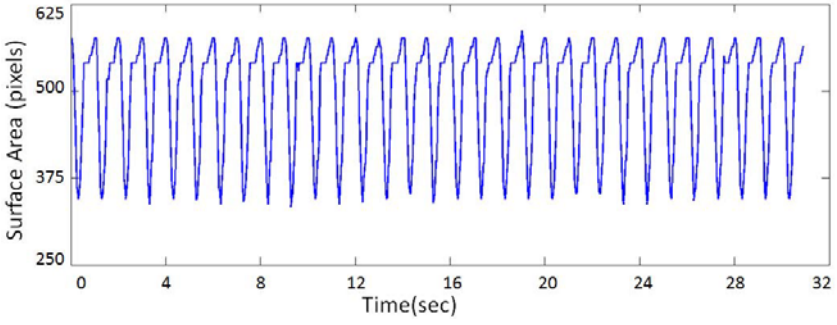

Fig. 3. Deformation mesh evolution signal for a CINE sequence

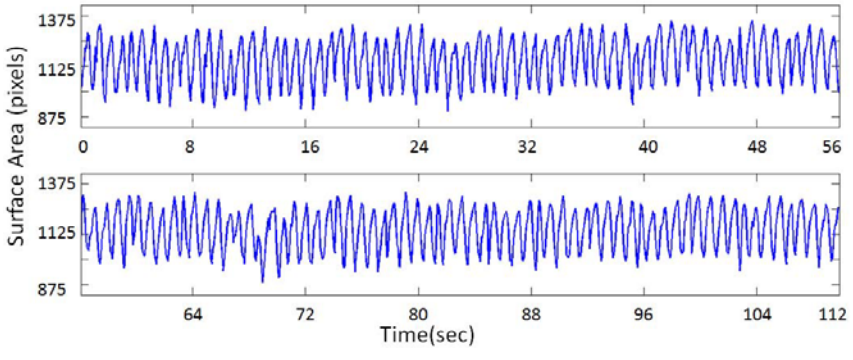

Fig. 4. Deformation mesh evolution signal for a true dynamic sequence. To fit the page, the long signal was split into two parts.

4 Conclusion

The superiority of the collaborative tracking algorithm [9] in long MRI sequences is demonstrated against a state of the art algorithm (MIL - [10]). The collaborative tracker excels in stable behavior and speed - both of paramount importance in interventional MRI. Furthermore, an algorithmic expansion introduced in the present article enables the computation of the deformed heart's surface through the cardiac cycle. The formed signal holds great potential not only as an interventional aid but also as a diagnostic tool. Specifically, this approach can be used for on-the-fly analysis of CINE (while the patient is still in the scanner), that is, for rapid extraction of hemodynamic or heart wall motion parameters. For example, it may provide valuable information about blood volume/velocity estimation and ejection fraction. Still, additional experimental studies are required to fully investigate the relationship of the deformation mesh signals to the hemodynamics of the LV.

Acknowledgements

This material is based upon work supported by the National Science Foundation (NSF) under grants No. #IIS-0812526 and #CNS-0932272. Any opinions, findings, and conclusions or recommendations expressed in this material are those of the authors and do not necessarily reflect the views of the funding agency.

References

1. Saikus, C.E., Lederman, R.J.: Interventional cardiovascular magnetic resonance imaging: A new opportunity for image-guided interventions. JACC Cardiovascular Imaging 2, 1321–1331 (2009)
2. Jolesz, F.A.: Future perspectives for intraoperative MRI. Neurosurgery Clinics of North America 16(1), 201–213 (2005)
3. Tsekos, N.V., Khanicheh, A., Christoforou, E., Mavroidis, C.: Magnetic resonance-compatible robotic and mechatronics systems for image-guided interventions and rehabilitation: A review study. Annual Review of Biomedical Engineering 9, 351–387 (2007)
4. McVeigh, E.R., Guttman, M.A., Lederman, R.J., Li, M., Kocaturk, O., Hunt, T., Kozlov, S., Horvath, K.A.: Real-time interactive MRI-guided cardiac surgery: Aortic valve replacement using a direct apical approach. Magnetic Resonance Medicine 56(5), 958–964 (2006)
5. Dowsey, A.W., Keegan, J., Lerotic, M., Thom, S., Firmin, D., Yang, G.: Motion-compensated MR valve imaging with COMB tag tracking and super-resolution enhancement. Medical Image Analysis 11(5), 478–491 (2007)
6. Spottiswoode, B.S., Zhong, X., Lorenz, C.H., Mayosi, B.M., Meintjes, E.M., Epstein, F.H.: 3D myocardial tissue tracking with slice followed cine DENSE MRI. Journal of Magnetic Resonance Imaging 27(5), 1019–1027 (2008)
7. Fradkin, M., Ciofolo, C., Mory, B., Hautvast, G., Breeuwer, M.: Comprehensive Segmentation of Cine Cardiac MR Images. In: Metaxas, D., Axel, L., Fichtinger, G., Székely, G. (eds.) MICCAI 2008, Part I. LNCS, vol. 5241, pp. 178–185. Springer, Heidelberg (2008)
8. Yuen, S.G., Kesner, S.B., Vasilyev, N.V., del Nido, P.J., Howe, R.D.: 3D Ultrasound-Guided Motion Compensation System for Beating Heart Mitral Valve Repair. In: Metaxas, D., Axel, L., Fichtinger, G., Székely, G. (eds.) MICCAI 2008, Part I. LNCS, vol. 5241, pp. 711–719. Springer, Heidelberg (2008)
9. Zhou, Y., Yeniaras, E., Tsiamyrtzis, P., Tsekos, N., Pavlidis, I.: Collaborative Tracking for MRI-Guided Robotic Intervention on the Beating Heart. In: Jiang, T., Navab, N., Pluim, J.P.W., Viergever, M.A. (eds.) MICCAI 2010. LNCS, vol. 6363, pp. 351–358. Springer, Heidelberg (2010)
10. Babenko, B., Yang, M.H., Belongie, S.: Visual tracking with online multiple instance learning. In: Proceedings of the IEEE Computer Society Conference on Computer Vision and Pattern Recognition, San Diego, California, pp. 983–990 (2009)